ICARUS 102, 107–116 (1993)

Modeling of S-Type Asteroid Spectra Using Primitive Achondrites and Iron Meteorites

TAKAHIRO HIROI

SN3, NASA Johnson Space Center, Houston, Texas 77058

JEFFREY F. BELL

Department of Geology and Geophysics, SOEST, University of Hawaii, Honolulu, Hawaii 96822

HIROSHI TAKEDA

Mineralogical Institute, Faculty of Science, University of Tokyo, Hongo, Tokyo 113, Japan

AND

CARLÉ M. PIETERS

Department of Geological Sciences, Brown University, Providence, Rhode Island 02912

Received July 7, 1992; revised November 30, 1992

The stony iron model for the S asteroids has been tested using observed reflectance spectra of the S asteroids and modeled spectra of meteoritic components. Observed reflectance spectra of 40 S asteroids were fit with linear combinations of laboratory reflectance spectra of 6 representative primitive achondrites and an iron meteorite. Specular and diffuse reflection components were taken into account for metallic-iron reflectance. Even with this limited set of meteorite spectra, 16 of those 40 S asteroids were fit fairly well in terms of absorption-band features and spectral profiles. The number of well-fit S asteroids may be greater if the number and variety of metallic and stony domains are expanded. This initial result suggests that many of the S-asteroidal surfaces may be various kinds of regional mixtures of primitive achondrites and metallic iron. If true, the S asteroids could have been originally formed of chondrite-like source materials because mineral assemblages of primitive achondrites seem to have recrystallized from chondrites by segregation of metallic components and loss of partial melts.

1. INTRODUCTION

The S asteroids are the most abundant asteroids in the inner main belt (Gradie and Tedesco 1982). Their visible and near-infrared reflectance spectra are interpreted to have characteristic features of stony irons and are different from spectra of ordinary chondrites (Chapman 1975, Gaffey and McCord 1978, Gaffey *et al.* 1989). Metallic iron in ordinary chondrites does not show the spectral reddening common for the S asteroids (Gaffey 1986), and the rotational variations of some S asteroids suggest that they may have mineralogical variation on their surfaces (Gaffey 1984). Fanale and Clark (1992) suggested that the S asteroids might be various kinds of intermediate materials between the M asteroids and chondritic materials. Recent calculations by Taylor (1992) suggest that complete differentiation of asteroids and the formation of distinct metallic cores is more difficult than previously believed and that partially differentiated asteroids with intimate mixtures of primitive silicates with metal are more common than their abundance among recovered meteorites.

Gaffey (1976) suggested that reflectance spectra of stony irons could be linearly synthesized from those of their individual mineralogical domains, which are usually several millimeters to one centimeter in size (the word "domain" in this paper is used to mean an optically isolated area of a single mineral or a particular intimate mixture of mineral grains). There had been few studies, however, that directly compared reflectance spectra between the S asteroids and stony irons in a wide wavelength range (0.3–2.6 μm), where mineral compositions can be best determined. The 52-color near-infrared survey by Bell *et al.* (1988) made such comparisons possible. Hiroi and Takeda (1991) showed that reflectance spectrum of an S

0019-1035/93 $5.00

asteroid (29 Amphitrite) was fit by a linear combination of an iron meteorite and a primitive achondrite.

The term "primitive achondrites" was first proposed by Prinz *et al.* (1983) for a group of meteorites that are mineralogically chondritic but have no chondrules. Many primitive achondrites have similar oxygen isotopic compositions (Clayton *et al.* 1992, Nagahara 1992), which suggests their common origin. Many primitive achondrites with near-chondritic chemistries and more reduced mafic silicates than those of chondrites have been grouped as acapulcoites (Clayton *et al.* 1992). Another group of primitive achondrites similar to Lodran are called lodranites. Lodran is a unique meteorite with abundant metallic iron, highly recrystallized olivine and orthopyroxene, but practically no augite or plagioclase (Bild and Wasson 1976). Some meteorites related to Winona and silicate inclusions in IAB and IIICD irons are also included in primitive achondrites.

In this paper, the earlier work of Hiroi and Takeda (1991) is expanded by using recently measured telescopic reflectance spectra of 40 S asteroids and laboratory spectra of 6 primitive achondrites and an iron meteorite. Based on the results of spectral fits and mineralogical studies of primitive achondrites, a possible common origin between the S asteroids and primitive achondrites is also discussed.

2. DESCRIPTION OF METEORITE SAMPLES

Y82111 is an H6 chondrite with highly recrystallized silicate grains and no visible chondrules (Hiroi and Takeda 1991). ALH77081 is an acapulcoite (Palme *et al.* 1981) and was studied mineralogically by Takeda *et al.* (1980). MAC88177, Y791491, and Y74357 are lodranites with considerable individual variations. MAC88177 is similar to Lodran but has a significant amount of augite (Takeda *et al.* 1991). Y791491 has not only augite but also a small amount of plagioclase (Hiroi and Takeda 1991) and is possibly paired with Y791493 (Nagahara and Ozawa 1986). Y74357 is an olivine-rich lodranite with some augite (Hiroi and Takeda 1991). The olivine grains in Y74357 show fractures decorated with fine metal and troilite particles. Those olivines are much more reduced than coexisting orthopyroxenes.

ALHA81187 is a unique meteorite described as similar to Acapulco, but the normal equilibrated texture of the primitive achondrites is disturbed, and fine subangular fragments (0.05–0.3 mm in diameter) of dusty mafic silicates are set in vein-like metal-rich matrices. In some areas, mafic silicates are more coarse-grained (up to 0.6 mm in diameter) and metals are more concentrated than in other areas. Curved grain boundaries of the original silicates are preserved in some silicate-rich areas. The orthopyroxene compositions in ALHA81187 are more reduced than in acapulcoites and are slightly zoned ($Ca_{2.6}Mg_{93}Fe_{4.4}$ to $Ca_{3.3}Mg_{89.5}Fe_{7.2}$). The most reduced compositions of orthopyroxene are nearly the same as those of olivine ($Fa_{3.7}$ to $Fa_{5.0}$). This range is close to those of winonaites, but is still greater than those of winonaites if we consider the Mg-richer values as due to reduction at later stages. A few Ca-poor pyroxene compositions suggest the occurrence of inverted protoenstatite.

TABLE I

Iron Contents of Olivines (Fa%) and Orthopyroxenes (Fs%) and Mineral Modal Abundances in Primitive Achondrites, Whose Reflectance Spectra Were Used in This Study

Primitive achondrites	Fa%	Fs%	Modal abundance (area %)				
			Ol	Opx	Aug	Pl	Metal etc.
Lodran[a]	14.8	13.1	37	35	0.1		28
MAC88177	13.0	12.0	39	44	6		11
Y791491	12.8	11.8	42	28	0.1	0.3	30
ALH77081	10.7	10.3	16	57	5	12	10
Y74357	7.9	13.8	83	6	3		8
ALHA81187	4.4	5.9	32	47	1	2	18

[a] Prinz (personal communications, 1982).

The iron contents of olivines (Fa%) and orthopyroxenes (Fs%) and mineral modal abundances of Lodran, MAC88177, Y791491, ALH77081, Y74357, and ALHA81187 are given in Table I. Those meteorites belong to a group of unique meteorites called primitive achondrites (Prinz *et al.* 1983). Shown in Fig. 1 are iron contents of olivines (Fa%) and orthopyroxenes (Fs%) in primitive achondrites. The silicates in primitive achondrites span a wide range of oxidation states, varying from the equiva-

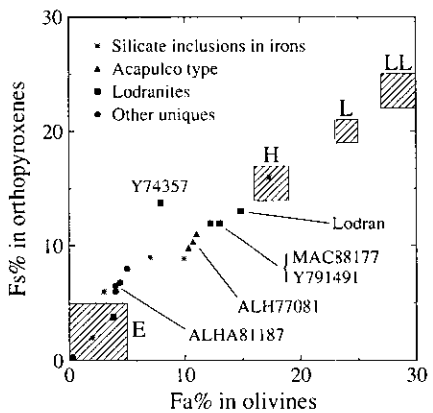

FIG. 1. Iron contents of olivines (Fa%) and orthopyroxenes (Fs%) in primitive achondrites plotted with those of equilibrated ordinary chondrites. Part of the data were compiled from Yanai and Kojima (1987), Score and Lindstrom (1990), Prinz *et al.* (1991), and Hiroi and Takeda (1991).

lent of E to H chondrites. Fa% and Fs% values are mostly close to their equilibrium relationships except for those of Y74357 and ALHA81187.

3. MEASUREMENTS OF REFLECTANCE SPECTRA

Near-infrared (0.8–2.6 μm) reflectance spectra of 40 S asteroids and two M asteroids were selected from the FCAS asteroid spectral survey (Bell *et al.* 1988). Ultraviolet–visible (0.3–1.1 μm) reflectance spectra of those asteroids can be found in Chapman and Gaffey (1979) except for 1866 Sisyphus. The visible (0.5–1.0 μm) reflectance spectrum of 1866 Sisyphus was taken from Vilas and McFadden (1992) and averaged to reduce noise. Visible and near-infrared reflectance spectra were combined by a scaling factor derived by the least-squares method.

Hemispherical reflectance spectra of a chip of H6 chondrite Y82111 was measured by Hiroi and Takeda 1991. Bidirectional reflectance spectra of chips of primitive achondrites (MAC88177, ALH77081, ALHA81187, Y74357, and Y791491) and crumbled Lodran were obtained using the RELAB facility with viewing geometry of 30° incidence and 0° emergence angles. Lodran had been naturally broken into smaller parts of millimeter scale. The details of RELAB are described in Pieters (1983) and in the RELAB Users Manual. Reflectance spectra of those six primitive achondrites are shown in Fig. 2a. These meteorites all show distinct spectral signatures of terrestrial alteration (rust) during the long times they spent in the Antarctic ice. This rusting is evident in the distinct iron oxide absorption bands near 0.50 and 0.65 μm and in the generally steep spectral slope in the visible wavelengths. The spectral effects of this alteration are small at wavelengths above 0.8 μm. A flat surface of iron meteorite Mundrabilla was roughened with No. 60 sandpaper, and its bidirectional reflectance spectrum was measured at "specular geometry" (15° incidence and 15° emergence) and "diffuse geometry" (30° incidence and 0° emergence). After treatment, the surface texture had features on the scale of 400 μm. Reflectance spectra obtained at those two geometries are shown in Fig. 2b. Specular geometry gives a much brighter and redder reflectance spectrum (see the detailed study by Britt and Pieters 1988).

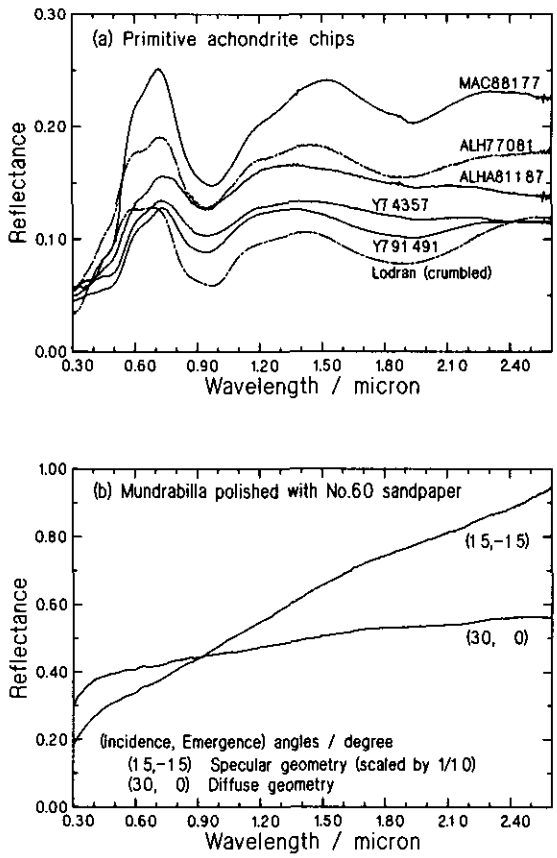

FIG. 2. Bidirectional reflectance spectra of meteorites used as end members for the spectral fittings of the S asteroids. (a) Six primitive achondrites at 30° incidence and 0° emergence angles. The Lodran sample had been naturally crumbled into particles down to 1 mm in size. All other samples were measured as chips. (b) Mundrabilla iron polished with No. 60 sandpaper. Reflectance at specular geometry is actually 10 times higher than shown.

4. METHOD OF FITTING

Shown in Fig. 3a are reflectance spectra of S asteroid 20 Massalia (Chapman and Gaffey 1979, Bell *et al.* 1988) compared with the general properties of iron meteorite Mundrabilla (diffuse geometry) and H6 chondrite Y82111. One can see that the spectral features of this particular asteroid are intermediate between those iron meteorite and H6 chondrite: curvature at 0.3–0.7 μm, absorption band depths at 0.9 and 1.9 μm, and overall redness. Because of this similarity a linear spectral fitting of this asteroid with those two meteorites was performed for a demonstration.

Reflectances of those meteorites were simply combined linearly at each wavelength, where the absolute reflectance of Massalia at 0.56 μm (c_0) and two linear combination coefficients (c_1 and c_2) were optimized to give the following relationship as close as possible:

$$c_0 R_S(\text{Massalia}) = c_1 R_A(\text{Mundrabilla}) + c_2 R_A(\text{Y82111}), c_1 + c_2 = 1, \quad (1)$$

where $R_S(\ )$ and $R_A(\ )$ indicate scaled and absolute reflectances of the material inside the parentheses, respectively. By dividing Eq. (1) by c_0, we obtain

$$R_S(\text{Massalia}) = C_1 R_A(\text{Mundrabilla}) + C_2 R_A(\text{Y82111}), C_1 + C_2 = 1/c_0. \quad (2)$$

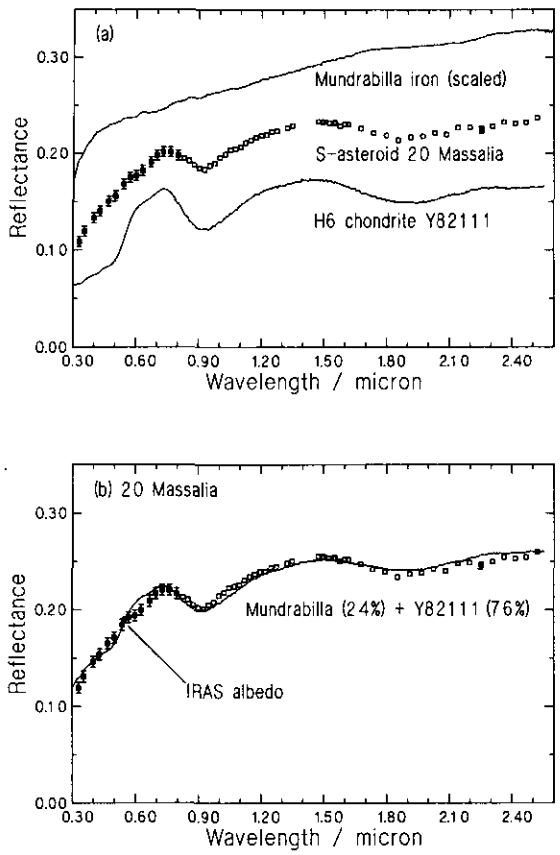

FIG. 3. The simplest example of a stony iron model for reflectance spectra of the S asteroids. (a) Reflectance spectra of S asteroid 20 Massalia compared with those of Mundrabilla iron (diffuse geometry) and H6 chondrite Y82111 (Hiroi and Takeda 1991). Reflectances of Mundrabilla and Massalia are scaled. (b) The result of a linear spectral fit of Massalia with Mundrabilla and Y82111. IRAS albedo is plotted as a filled circle at 0.55 μm, which is almost equal to the optimized albedo.

First C_1 and C_2 in Eq. (2) were optimized independently, and then c_0, c_1, and c_2 were calculated by

$$c_0 = 1/(C_1 + C_2), \quad c_1 = c_0 C_1, \quad c_2 = c_0 C_2. \qquad (3)$$

The result is shown in Fig. 3b. The optimized absolute reflectance of Massalia is very close to the IRAS albedo 19% (Tedesco 1989) shown as a filled circle. Although the IRAS model geometric albedoes are not directly comparable with the absolute bidirectional reflectance at 0.55 μm measured in laboratories, they are given to check if there is any systematic relationship between those two. A linear combination of two reflectance spectra mathematically corresponds to a regional mixing of those two materials if the scale of mixing is larger than the optical skin depth of those materials. Silicate domains in stony iron meteorites are usually larger than their optical skin depth, which is of millimeter scale.

This simple linear fitting was expanded in two respects to fit various kinds of S-asteroidal reflectance spectra. (1) We assume that S-type asteroids can have surfaces on which several different kinds of stony domains are exposed, as is shown in Fig. 4. Each of these stony domains was assumed to be an intimate mixture of mineral grains similar to one of the primitive achondrites. Reflectance spectra of those stony domains were approximated with bidirectional reflectance spectra of six representative primitive achondrites (Fig. 2a), which were measured at one viewing geometry because the spectral shape of silicate minerals are not highly dependent on viewing geometry. (2) Different viewing geometries were taken into account for the metallic domain because reflectance of a metallic iron surface changes greatly in brightness and spectral shape depending on its viewing geometry. Reflectance spectra of Mundrabilla iron at diffuse and specular geometries (Fig. 2b) were combined linearly to approximate various ratios of specular and diffuse components of reflected light. This procedure allows for the existence of differing regolith structures and particle size distributions on S-type asteroids.

Reflectance spectra of all the primitive achondrites and Mundrabilla were initially used as components for fitting of each asteroidal reflectance spectrum. Their linear combination coefficients and the asteroidal albedo were optimized by a least-squares method, and components with negative coefficients were removed. The optimization were repeated until all the coefficients become positive except for specular geometry of Mundrabilla. A negative contribution was allowed for this spectrum because of our very poor knowledge of the surface microstructure of metal surfaces on asteroids.

5. RESULTS OF FITTING

First of all, the validity of using reflectance spectra of Mundrabilla iron was tested with spectra of two M

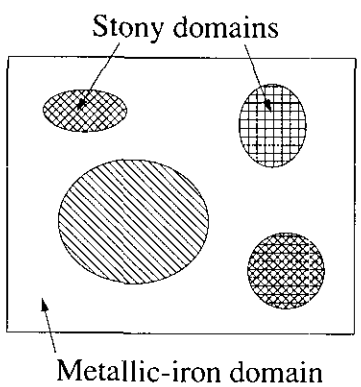

FIG. 4. A stony iron model for reflectance spectra of the S asteroids. Hatched areas indicate various kinds of stony domains, each of which is an intimate mixture of mineral grains.

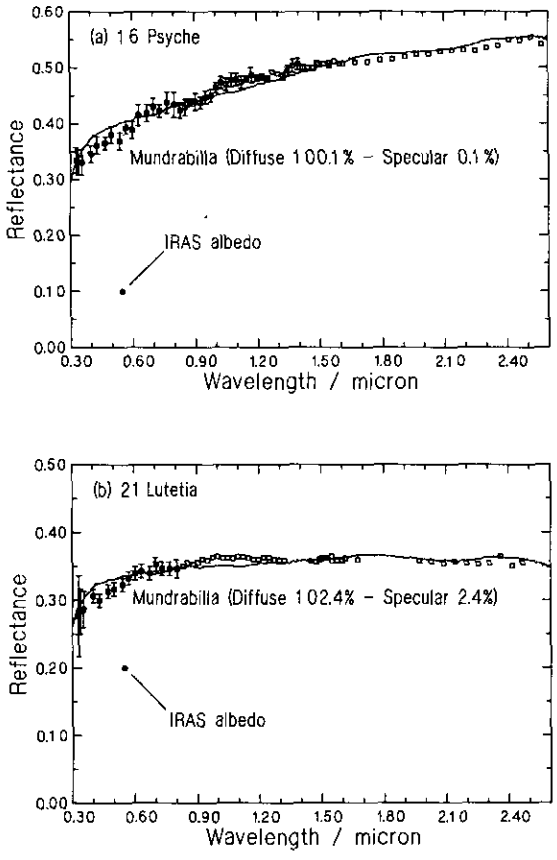

FIG. 5. Linear spectral fits of the M asteroids, (a) 16 Psyche and (b) 21 Lutetia, with specular and diffuse geometries of Mundrabilla iron. IRAS albedoes (Tedesco 1989) are plotted as filled circles for comparison.

asteroids. Shown in Fig. 5 are the linear spectral fits of M asteroids 16 Psyche and 21 Lutetia (Chapman and Gaffey 1979, Bell *et al.* 1988) with Mundrabilla iron at diffuse and specular geometries. Those results show that 16 Psyche is well approximated by Mundrabilla iron at its diffuse viewing geometry, whereas 21 Lutetia has more diffuse component of reflected light than diffuse geometry (30° incidence and 0° emergence angles). Only 2% difference of specular geometry area made such large differences in brightness and redness of reflectance spectra because specular geometry gives reflectance about 10 times higher than diffuse geometry (Fig. 2b).

Linear spectral fittings of 40 S asteroids with six primitive achondrites and Mundrabilla iron (diffuse and specular geometries) were performed. Those results are listed in Table II. Root mean square deviations (RMSD) of those fits were calculated relative to the optimized albedoes. The "best-fit" S asteroids were selected by considering both their relative errors (4% or less) and visual impressions such as absorption-band features and spectral profiles. In all, 16 asteroids (marked with open circles in Table II) were selected. Those best-fit asteroids have metallic iron domains up to 37% in area. This estimation of metallic iron area may change depending on what kind of meteorites are used as end members for the spectral fittings. The number of best-fit S asteroids could increase if a greater variety of reflectance spectra for metallic and stony domains are used. The observed (scaled) and calculated reflectance spectra of best-fit S asteroids are shown in Fig. 6.

6. ORIGIN OF THE S ASTEROIDS AND PRIMITIVE ACHONDRITES

The advantage of using primitive achondrites instead of ordinary chondrites to study the S asteroids is that primitive achondrites have the same mineral species but much more variety than ordinary chondrites in terms of their mineralogy, especially the amount of metallic iron. As the result, primitive achondrites have a large spectral variation within the group in spite of the small number of available meteorites compared with ordinary chondrites. The S asteroids also have a large spectral variation within the group. The simplest interpretation of the results of spectral fittings, is that primitive achondrites may be the fragments stripped off from stony domains of the S asteroids. The fact that primitive achondrites often exist as inclusions in iron meteorites (Prinz *et al.* 1983) also supports that idea.

Olivines in Y74357 and ALHA81187 are much more reduced than their coexisting orthopyroxenes (Table I and Fig. 1) and are full of fractures decorated by fine metal and troilite particles. This suggests that Y74357 and ALHA81187 may have experienced both shock and annealing processes that reduced its olivines, whereas its orthopyroxenes remained less reduced due to their slower Fe–Mg interdiffusion during cooling (Hiroi and Takeda 1991). Six primitive achondrites used in this study each have unique features distinguished by iron contents of their silicates, olivine/orthopyroxene ratios, presence or absence of minor minerals such as augite and plagioclase, metallic iron abundances, and shock and annealing textures. Each of them may represent different stages or types of alteration from the common source material on their parent body. Alternatively, they may represent different locations in the same general area of the solar nebula.

Recent work on the behavior of magmas under asteroidal conditions (Taylor 1992) shows that substantial amounts of melting (~50%) are required for metal in a chondritic body to drain away and form a core. The primitive achondrites, and similar stony iron meteorites, probably represent samples from asteroids which were not heated sufficiently to reach this level of melting. The metallic iron which failed to settle into a core

TABLE II
Results of Linear Spectral Fits of 40 S Asteroids with Mundrabilla Iron and 6 Primitive Achondrites.

S asteroids	Albedo% IRAS*	Albedo% Fit	RMSD% Absolute	RMSD% Relative		Mundrabilla % Specular	Mundrabilla % Diffuse	Primitive achondrites % MAC88177	ALH77081	ALHA81187	Y74357	Y791491	Lodran
3 Juno	22	21.0	0.56	2.7	o	-0.36	32.46	8.50	24.77	34.64			
5 Astraea	14	16.5	0.62	3.7		0.15	16.90		81.88			1.07	
6 Hebe	25	19.6	0.42	2.1	o	0.11	23.51		6.94	69.45			
7 Iris	21	21.1	0.59	2.8	o	0.49	22.86	15.31	18.66	42.69			
9 Metis		23.5	1.07	4.5		1.15	25.26	10.37		63.22			
11 Parthenope	15	20.9	0.43	2.1	o	0.57	22.93		22.21	54.29			
12 Victoria	16	23.7	1.31	5.5		2.57	12.21	0.70		84.53			
15 Eunomia	19	26.7	0.90	3.4		0.64	37.31	36.65		25.40			
18 Melpomene	22	20.8	0.63	3.0	o	1.02	19.44		5.26	74.28			
20 Massalia	19	18.5	0.42	2.2		0.11	23.90			51.18		18.71	6.10
25 Phocaea	22	22.3	1.03	4.6		1.69	14.51	25.94		57.87			
26 Proserpina	16	18.8	0.69	3.7		0.12	20.79	9.23		69.86			
27 Euterpe		20.2	0.66	3.2		0.70	17.79	20.44		61.07			
29 Amphitrite	16	21.7	0.39	1.8	o	0.26	33.14		3.53	63.07			
32 Pomona	25	19.3	0.39	2.0	o	-0.01	26.01		0.43	60.53			13.05
37 Fides	17	21.7	0.54	2.5	o	1.00	22.92	3.78	3.18	39.46	14.33		15.34
39 Laetitia	29	21.7	0.77	3.5		1.06	18.09	21.38		59.46			
40 Harmonia	20	18.0	0.42	2.3		0.51	16.18			83.31			
42 Isis	12	22.2	1.03	4.6		1.50	17.57	11.46		69.47			
43 Ariadne	28	23.2	0.73	3.1	o	-0.70	37.52	33.61	29.56				
63 Ausonia	17	21.6	0.89	4.1		2.58	1.20	29.18		67.04			
68 Leto	20	23.1	1.52	6.6		0.56	25.46	35.45		38.53			
80 Sappho	15	20.8	0.71	3.4	o	1.29	8.59	20.26	12.92	56.95			
82 Alkmene	17	15.4	0.55	3.6	o	-0.18	17.82			56.79		25.58	
89 Julia	16	19.9	0.83	4.2		0.75	20.45			78.80			
113 Amalthea	27	29.1	2.13	7.3		0.92	36.14	62.94					
115 Thyra	25	21.7	0.51	2.4	o	-0.57	35.73	33.42		5.46	24.94		1.02
116 Sirona	22	19.8	0.85	4.3		0.31	26.19		1.85	59.68			11.96
221 Eos	12	21.9	1.21	5.5		-0.77	36.76		38.33	25.68			
258 Tyche	15	17.8	0.61	3.4	o	0.80	13.85			63.39	13.97		7.99
264 Libussa	27	16.5	1.00	6.1		0.86	10.74			88.39			
354 Eleonora	19	29.9	2.13	7.1		2.25	20.85	76.90					
389 Industria	20	21.5	0.52	2.4	o	0.07	31.83		9.39	57.28			1.44
532 Herculina	16	24.3	0.73	3.0	o	0.78	27.09	21.26	17.27	33.62			
584 Semiramis	17	35.4	1.64	4.6		3.09	32.42	64.49					
639 Latona		29.5	1.51	5.1		2.32	35.08	4.77		57.84			
674 Rachele	18	17.9	0.47	2.6		0.34	17.92			81.75			
714 Ulula	24	19.2	1.79	9.3		0.56	18.74	3.27		77.43			
1036 Ganymed	17	14.7	0.741	5.0		0.56	4.78			68.85			25.81
1866 Sisyphus		23.6	0.392	1.7	o	1.58	9.51	7.47		81.44			

Note. Root mean square deviations (RMSD) are given, while 16 best fits (marked with open circles) were chosen based on their visual impressions.

* Tedesco (1989).

may have formed subsurface metallic iron networks surrounding isolated domains of silicates. Further destruction of the asteroids could have been difficult due to the stronger binding force of their metallic iron networks, which can explain the extremely small population of primitive achondrites in our meteorite collections (Bell 1991). If those asteroids are the S asteroids that are presently abundant in the inner main belt, the absence of chondritic asteroids at the larger scales can be explained. Only smaller asteroids could have remained unaltered from their original materials, which may have been similar to ordinary chondrites (Bell *et al.* 1989, Bell and Keil 1988).

The oxygen isotopic compositions of most of primitive achondrites used in this study, are different from those of ordinary chondrites and are very close to one another (Clayton *et al.* 1992, Nagahara 1992). It suggests that primitive achondrites may have come from one region of the solar nebula, which is different from the region where ordinary chondrites formed. Therefore, if primitive

FIG. 6. Results of linear spectral fits of 40 S asteroids with six primitive achondrites and Mundrabilla iron at specular and diffuse geometries. Reflectance spectra of the S asteroids are taken from Chapman and Gaffey (1979) and Bell *et al.* (1988) except for the visible range of 1866 Sisyphus from Vilas and McFadden (1992).

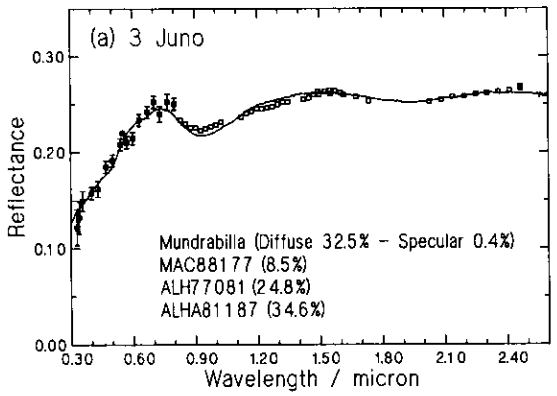
(a) 3 Juno
Mundrabilla (Diffuse 32.5% – Specular 0.4%)
MAC88177 (8.5%)
ALH77081 (24.8%)
ALHA81187 (34.6%)
Reflectance
Wavelength / micron

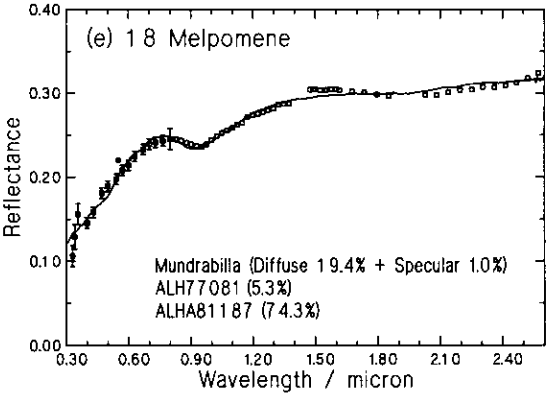
(e) 18 Melpomene
Mundrabilla (Diffuse 19.4% + Specular 1.0%)
ALH77081 (5.3%)
ALHA81187 (74.3%)
Reflectance
Wavelength / micron

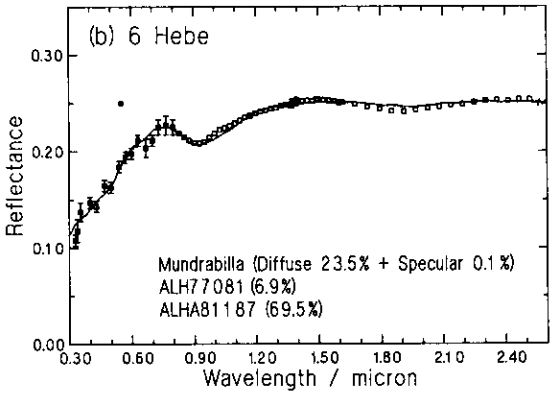
(b) 6 Hebe
Mundrabilla (Diffuse 23.5% + Specular 0.1%)
ALH77081 (6.9%)
ALHA81187 (69.5%)
Reflectance
Wavelength / micron

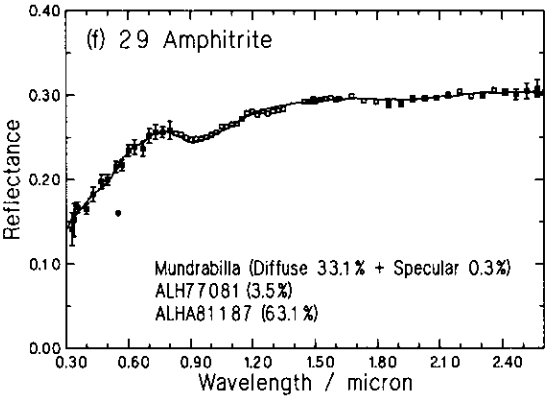
(f) 29 Amphitrite
Mundrabilla (Diffuse 33.1% + Specular 0.3%)
ALH77081 (3.5%)
ALHA81187 (63.1%)
Reflectance
Wavelength / micron

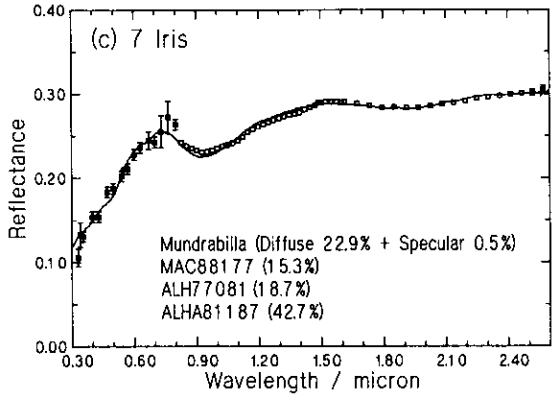
(c) 7 Iris
Mundrabilla (Diffuse 22.9% + Specular 0.5%)
MAC88177 (15.3%)
ALH77081 (18.7%)
ALHA81187 (42.7%)
Reflectance
Wavelength / micron

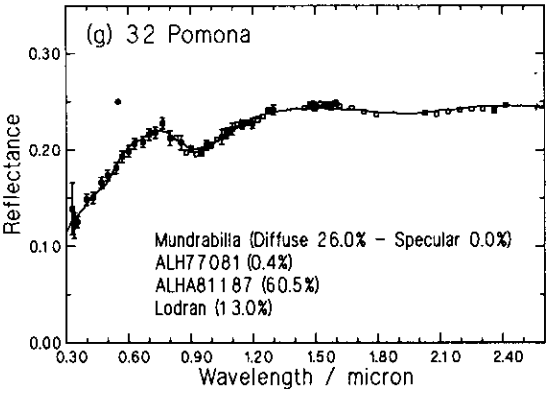
(g) 32 Pomona
Mundrabilla (Diffuse 26.0% – Specular 0.0%)
ALH77081 (0.4%)
ALHA81187 (60.5%)
Lodran (13.0%)
Reflectance
Wavelength / micron

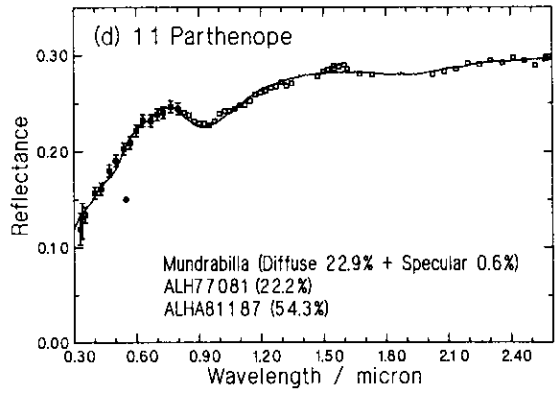
(d) 11 Parthenope
Mundrabilla (Diffuse 22.9% + Specular 0.6%)
ALH77081 (22.2%)
ALHA81187 (54.3%)
Reflectance
Wavelength / micron

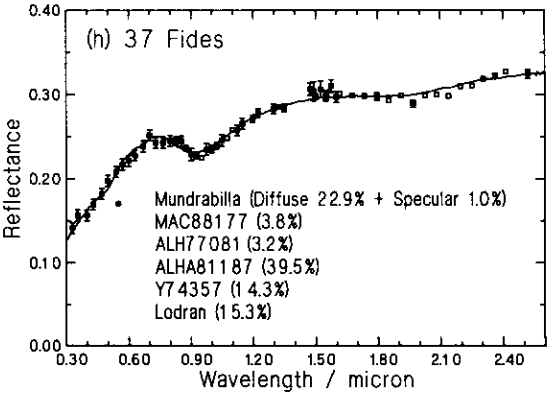
(h) 37 Fides
Mundrabilla (Diffuse 22.9% + Specular 1.0%)
MAC88177 (3.8%)
ALH77081 (3.2%)
ALHA81187 (39.5%)
Y74357 (14.3%)
Lodran (15.3%)
Reflectance
Wavelength / micron

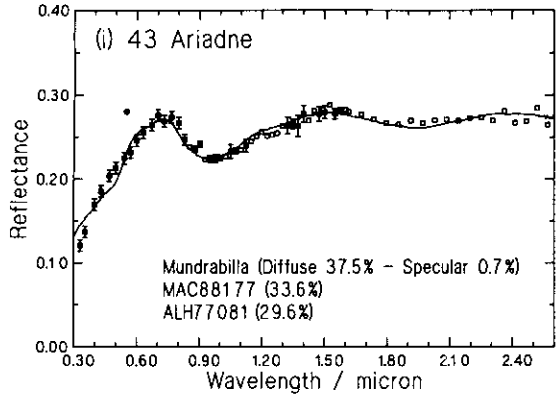

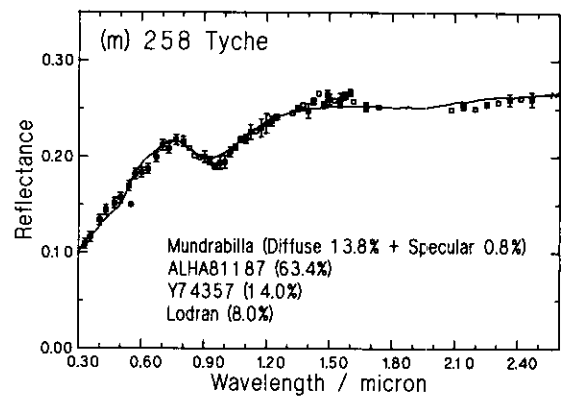

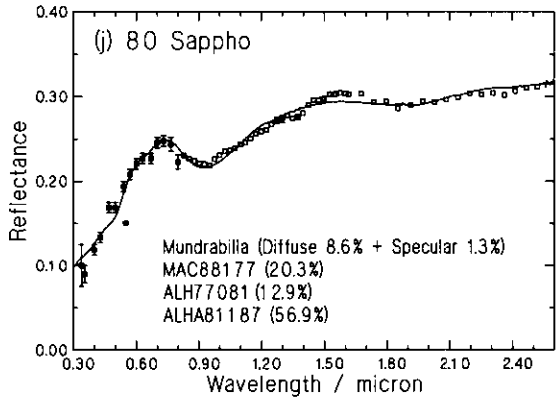

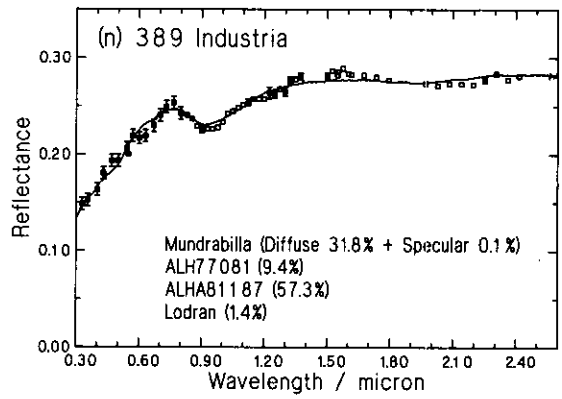

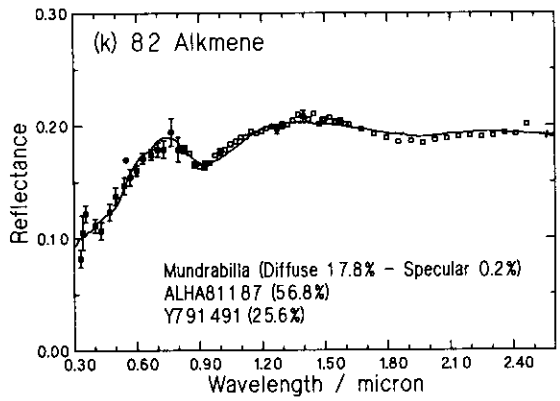

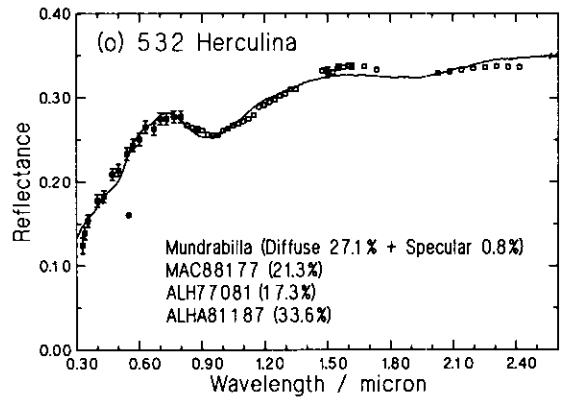

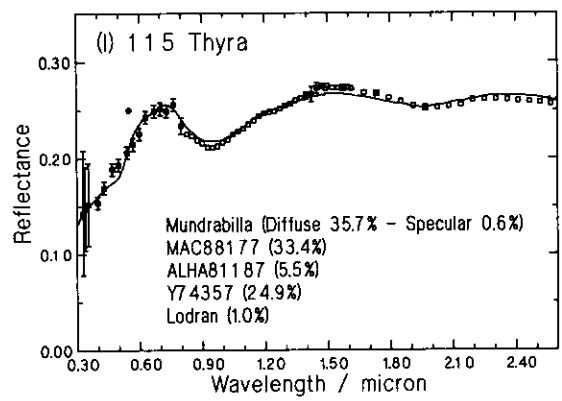

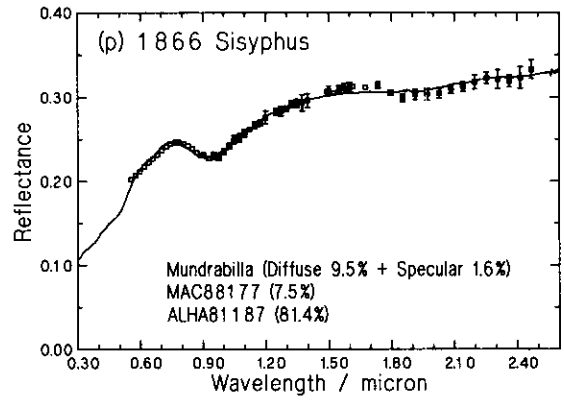

FIG. 6—*Continued*

achondrites came from the S asteroids, ordinary chondrites that fell onto the earth must have come from some other kind of parent bodies.

A serious remaining problem is that we have little information on the effects of regolith processes on stony iron asteroids due to the lack of stony iron regolith breccias. Such breccias are common among basaltic achondrites and all classes of chondrites and have provided valuable insight into proposed spectral alteration processes on such bodies. Their absence among irons and stony irons is frustrating and leaves room for considerable speculation on the nature (or even existence) of regoliths on M-type and S-type asteroids.

7. CONCLUSIONS

(1) Forty percent of well-measured reflectance spectra of the S asteroids can be fit by a stony iron model composed of an iron meteorite and six representative primitive achondrites. Probably most S asteroid spectra could be reproduced by increasing the number of meteorites measured and allowing for intimate mixing between meteorite types.

(2) The hypothesis that the S asteroids are composed of primitive achondrites strongly bound together by metallic iron networks can explain the extremely small population of primitive achondrites in our meteorite collections.

(3) If all the larger asteroids initially formed of ordinary chondrite-like source materials were altered to the S asteroids, the apparent absence of ordinary chondrites in the main belt may be due to the fact that they are too small to have their reflectance spectra measured.

ACKNOWLEDGMENTS

We thank Faith Vilas for reflectance data for asteroid 1866 Sisyphus and helpful discussions. We also thank the National Institute of Polar Research for chips of Y74357 and Y791491, the Meteorite Working Group for chips of MAC88177 and ALHA81187, and the American Museum of Natural History for Lodran. Reflectance spectra of primitive achondrites were measured at RELAB in Brown University. We thank S. F. Pratt for those measurements. RELAB is a multiuser facility supported by NASA under Grant NAGW-748. We also thank Lucy McFadden and Dan Britt for their constructive comments to the manuscript. This work was done while one of the authors (T. Hiroi) held a National Research Council–NASA/JSC Research Associateship.

REFERENCES

BELL J. F. 1991. Size-dependent composition in interplanetary material. *Bull. Am. Astron. Soc.* **23,** 1140.

BELL, J. F., P. D. OWENSBY, B. R. HAWKE, AND M. J. GAFFEY 1988. The 52-color asteroid survey: Final results and interpretation. *Lunar Planet. Sci.* **19,** 57–58.

BELL, J. F., AND K. KEIL 1988. Spectral alteration effects in chondritic regolith breccias. *Proc. Lunar Planet. Sci. Conf.* 18th, 573–580.

BELL, J. F., D. R. DAVIS, W. K. HARTMANN, AND M. J. GAFFEY 1989. Asteroids: The big picture. In *Asteroids II* (R. P. Binzel, T. Gehrels, and M. S. Matthews, Eds.), pp. 921–945. Univ. of Arizona Press, Tucson.

BILD, R. W., AND J. T. WASSON 1976. The Lodran meteorite and its relationship to the ureilities. *Mineral. Mag.* **40,** 721–735.

BRITT, D. T., AND C. M. PIETERS 1988. Bidirectional reflectance properties of iron–nickel meteorites. *Proc. Lunar Planet. Sci. Conf.* 18th, 503–512.

CHAPMAN, C. R. 1975. The nature of asteroids. *Sci. Am.* **232(1),** 24–33.

CHAPMAN, C. R., AND M. J. GAFFEY 1979. Reflectance spectra for 277 asteroids. In *Asteroids* (T. Gehrels, Ed.), pp. 1064–1089. Univ. of Arizona Press, Tucson.

CLAYTON, R. N., T. K. MAYEDA, AND H. NAGAHARA 1992. Oxygen isotope relationships among primitive achondrites. *Lunar Planet. Sci.* **23,** 231–232.

FANALE, F. P., AND B. E. CLARK 1992. BAR plot analysis of S type asteroid and ordinary chondrite reflectance spectra. *Lunar Planet. Sci.* **23,** 345–346.

GAFFEY, M. J. 1976. Spectral reflectance characteristics of the meteorite classes. *J. Geophys. Res.* **81,** 905–920.

GAFFEY, M. J. 1984. Rotational spectral variations of asteroid (8) Flora: Implications for the nature of the S-type asteroids and for the parent bodies of the ordinary chondrites. *Icarus* **60,** 83–114.

GAFFEY, M. J. 1986. The spectral and physical properties of metal in meteorite assemblages: Implications for asteroid surface materials. *Icarus* **66,** 468–486.

GAFFEY, M. J., AND T. B. MCCORD 1978. Asteroid surface materials: Mineralogical characterizations from reflectance spectra. *Space Sci. Rev.* **21,** 555–628.

GAFFEY, M. J., J. F. BELL, AND D. P. CRUIKSHANK 1989. Reflectance spectroscopy and asteroid surface mineralogy. In *Asteroids II* (R. P. Binzel, T. Gehrels, and M. S. Matthews, Eds.), pp. 98–127. Univ. of Arizona Press, Tucson.

GRADIE, J., AND E. TEDESCO 1982. Compositional structure of the asteroid belt. *Science* **216,** 1405–1407.

HIROI, T., AND H. TAKEDA 1991. Reflectance spectroscopy and mineralogy of primitive achondrites–lodranites. *Proc. NIPR Symp. Antarct. Meteorites* **4,** 163–177.

NAGAHARA, H. 1992. Yamato-8002: Partial melting residue on the "unique" chondrite parent body. *Proc. NIPR Symp. Antarct. Meteorites* **5,** 191–223.

NAGAHARA, H., AND K. OZAWA 1986. Petrology of Yamato-791493, "lodranite": Melting, crystallization, cooling history, and relationship to other meteorites. *Mem. Natl. Inst. Polar Res., Special Issue* **41,** 181–205.

PALME, H., L. SCHULTZ, B. SPETTEL, H. W. WEBER, H. WÄNKE, M. C. MICHEL-LEVY, AND J. C. LORIN 1981. The Acapulco meteorite: Chemistry, mineralogy and irradiation effects. *Geochim. Cosmochim. Acta* **45,** 727–752.

PIETERS, C. M. 1983. Strength of mineral absorption features in the transmitted component of near-infrared reflected light: First results from RELAB. *J. Geophys. Res.* **88,** 9534–9544.

PRINZ, M., C. E. NEHRU, J. S. DELANEY, AND M. WEISBERG 1983. Silicates in IAB and IIICD irons, winonaites, lodranites and Brachina: A primitive and modified-primitive group. *Lunar Planet. Sci.* **14,** 616–617.

PRINZ, M., N. CHATTERJEE, M. K. WEISBERG, R. N. CLAYTON, AND T. K. MAYEDA 1991. Silicate inclusions in Antarctic irons. *Lunar Planet. Sci.* **22,** 1101–1102.

SCORE, R., AND M. M. LINDSTROM 1990. *Antarct. Meteorite Newsl.* **13(1).**

TAKEDA, H. 1989. Mineralogy of coexisting pyroxenes in magnesian ureilities and their formation conditions. *Earth Planet. Sci. Lett.* **93,** 181–194.

TAKEDA, H., J. SAITO, M. MIYAMOTO, AND T. HIROI 1991. Mineralogy of MAC88177 and comparison with augite-bearing lodranite, Yamato 74357. *Lunar Planet. Sci.* **22,** 1375–1376.

TAYLOR, G. J. 1992. Core formation in asteroids. *J. Geophys. Res.* **97,** 14,717–14,726.

TEDESCO, E. F. 1989. Asteroid magnitudes, UBV colors, and IRAS albedos and diameters. In *Asteroids II* (R. P. Binzel, T. Gehrels, and M. S. Matthews, Eds.), pp. 1090–1138. Univ. of Arizona Press, Tucson.

VILAS, F., AND L. A. MCFADDEN 1992. CCD reflectance spectra of selected asteroids: Presentation and data analysis considerations. *Icarus* **100,** 85–94.

YANAI, K., AND H. KOJIMA 1987. *Photographic Catalog of the Antarctic Meteorites*. National Institute of Polar Research, Tokyo, Japan.